Taylor & Francis
Taylor & Francis Group

Particulate Science and Technology

An International Journal

ISSN: 0272-6351 (Print) 1548-0046 (Online) Journal homepage: http://www.tandfonline.com/loi/upst20

Multiscale modeling of nonequilibrium gas–liquid mixture flows in phase transition regions

Rakiz M. Sattarov, George S. Dulikravich & Ilham R. Sattarzada

To cite this article: Rakiz M. Sattarov, George S. Dulikravich & Ilham R. Sattarzada (2017): Multiscale modeling of nonequilibrium gas–liquid mixture flows in phase transition regions, Particulate Science and Technology, DOI: 10.1080/02726351.2017.1305025

To link to this article: http://dx.doi.org/10.1080/02726351.2017.1305025

Accepted author version posted online: 23 Mar 2017.
Published online: 23 Mar 2017.

Submit your article to this journal

Article views: 13

View related articles

View Crossmark data

Full Terms & Conditions of access and use can be found at
http://www.tandfonline.com/action/journalInformation?journalCode=upst20

Download by: [69.247.250.149] **Date:** 29 April 2017, At: 06:52

PARTICULATE SCIENCE AND TECHNOLOGY
http://dx.doi.org/10.1080/02726351.2017.1305025

Taylor & Francis
Taylor & Francis Group

Multiscale modeling of nonequilibrium gas–liquid mixture flows in phase transition regions

Rakiz M. Sattarov[a], George S. Dulikravich[b], and Ilham R. Sattarzada[c]

[a]Scientific-Engineering Company, BEC, Baku, Azerbaijan; [b]Department of Mechanical & Materials Eng., MAIDROC Lab., Florida International University, Miami, FL, USA; [c]Fluor Enterprises Inc., Sugar Land, TX, USA

ABSTRACT

This paper presents multiscale modeling substantiated with experimental aspects of state, filtration, and motion of the gas–liquid mixtures involving phase transition regions in concentrated volumes applicable to porous media and pipe flows. Based on physics, it is confirmed analytically that actual levels of underpressure in gas–liquids systems are considerably above traditional understanding of saturation pressure at which gas emission from the liquid and its dissolution in the liquid in a form of embryos can occur. It is demonstrated that these processes are not equilibrium processes, and they can also occur on nanoscales and microscales. Thermo-hydrodynamic analyses and experimental investigation of the gas–liquid systems in areas of phase transition presented here have resulted in useful equations governing such flows in filtration in the porous media and in straight pipes.

KEYWORDS

Disperse systems; gas–liquid systems; inhomogeneous complex fluids; micro-embryonic elements; nanoelements; phase transition regions

1. Introduction

Monitoring and management of technological processes involving fluids usually require modeling of motion of structured heterogeneous liquids, which are characterized by complex physicochemical and thermodynamic properties. Flows of such heterogeneous complex fluids are commonly defined by the capillary and molecular surface properties on interphase boundaries either between fluids or solid–liquid interface (Mirzadzhanzade et al. 1985; Mirzadzhanzade, Hasanov, and Bahtizin 1999; Sattarov 1999, 2016; Houshmand et al. 2014). Probably the most important filtration and hydraulic characteristics of inhomogeneous liquids are wettability and also the phenomenon of ion exchange between phases and multiphase systems with a solid surface. It should be noted that inhomogeneous heterogeneous complex fluids are disperse systems, as a rule, with aggregative stable structures and increases of concentration of dispersed phases that makes particles interact in a way similar to associations of molecules and ions (Mirzadzhanzade et al. 1985; Mirzadzhanzade, Hasanov, and Bahtizin 1999; Sattarov 1999, 2012; Frolov 1982; Clasen and McKinley 2004). This phenomenon can especially show itself in gas–liquids systems when underpressure is considerably above traditional understanding of saturation pressure at which point gas emission from the liquid and its dissolution in the liquid in a form of nano- and microsized embryos occur, which essentially change a condition of the gas–liquids systems and demands of new approach to mathematical modeling of this process.

Filtration and hydraulic characteristics are characterized by regulation of ion exchange and electric charge processes, wettability, dispersion of phases, physical and chemical composition of reagents in inhomogeneous systems, different additives of chemical reagents and by action of physical fields. This means that regulation processes, especially in phase transition regions, need to be understood as control lows of flow of inhomogeneous complex fluids in porous media and pipes on nanoscales or microscales. This means that purposeful regulation of processes or properties of inhomogeneous complex fluids on molecular or supramolecular levels defines the physical and chemical phenomena and parameters that are considered to be the most influential during modeling of systems and processes at nanoscales or microscales (Havkin 2007; Sattarov et al. 2010, 2012). In this respect, mathematical models of control of technological processes by application of chemical, physical, thermal, and other methods of action should be based on modeling of flow of inhomogeneous complex fluids especially in their phase transition regions.

In addition to some of the existing assumptions, it must be understood that causes and mechanisms of the formation of dynamically stable nano- or microembryos are not yet fully established. Also lacking are reliable models of complex systems of nonhomogeneous flow in the pretransition and the transition of saturation areas.

Based on what was stated above, this paper analyzes features of phase transformations and offers model features of some processes in filtration and flow in pipes of various inhomogeneous gas–liquid complex systems in phase transition regions under saturation pressure and above.

2. Flow of gas–liquid mixtures in phase transition regions

Mechanisms of filtration and flow of gas–liquid mixtures in the real porous media and pipes, along with their parameters,

CONTACT George S. Dulikravich dulikrav@fiu.edu Department of Mechanical & Materials Eng., MAIDROC Lab., Florida International University, 10555 West Flagler Street, Miami, Florida 33174, USA.

© 2017 Taylor & Francis

are strongly influenced by the thermodynamic properties of the multiphase systems (Mirzadzhanzade et al. 1999; Sattarov 1999). One of the most important indicators of dispersed systems is effective viscosity, which, particularly for gas–liquid systems, depends on many factors, such as temperature, pressure, and concentration of the dispersed phase. The most widespread model of dependence of the effective viscosity μ on concentration was published by Einstein (1966). He stated that in case of a suspension of fine rigid particles in a liquid when viscosity coefficient of the rigid particles' material is infinitely larger than the viscosity coefficient of the liquid, the effective viscosity coefficient of such a suspension (mixture) is

$$\mu = \mu_0(1 + 2.5C). \tag{1}$$

This relation was obtained on the basis of the hypothesis that infinitely many identical minuscule solid inclusions of spherical shape are randomly distributed in the viscous fluid having viscosity coefficient, μ_0. The solid inclusions radii are so small that the entire volume they occupy is significantly less than continuum volume. Moreover, values of the effective hydrodynamic diameter of molecules, under certain conditions, are conforming to the value of nanosizes set to 10^{-9} m.

Einstein also stated that in case of a homogeneous suspension of gas bubbles in a liquid when viscosity coefficient of the gas bubbles material is infinitely smaller than the viscosity coefficient of the liquid, the effective viscosity coefficient of such a liquid–gas or liquid–vapor mixture obeys the same Equation (1), except that the coefficient value should be changed from 2.5 to 1.0.

However, even when using the constant coefficient 1.0 in Equation (1) for gas–liquid systems, the resulting effective coefficient of viscosity of the mixture does not match well with experimental data. For example, in cases when utilized pressure is higher than saturation pressure, effective viscosity for the gas-liquid mixture does not increase with scaling up a concentration of gas microparticles as predicted by Einstein's model. On the contrary, the effective viscosity then decreases.

Of particular interest is the situation when the gas–liquid mixture is subject to normal and higher saturation pressures. In such situations, gas emission from the liquid and its dissolution in the liquid occur in a form of embryos (microscopically small gas bubbles), around which continues further growth of a new phase (Frenkel 1975). This newly created phase at the initial stage of the process is a nanoparticle or a cluster of nanoparticles, which have smaller sizes than ordinary microscopic inclusions in the aggregate state of the relevant phase. In this situation, an equilibrium between the phases for either gas-saturated liquid or condensable gas will be unstable, meaning that insignificant changes in the radii of the newly incipient phase will cause changes in pressure of a phase transition, which is different from a pressure of the main phase. Consequently, the new phase either begins to return to its initial state or its size continues to grow.

Some research results (Sattarov and Farzane 1987) of the gas–liquid systems in a sufficiently wide range of pressure change have shown that value of effective viscosity in the regions of higher and lower pressures than saturation pressure is changing considerably, following minor changes of pressure and temperature. It is possible to explain this effect by the influence of the emerging microembryos of gas inclusions under the conditions of normal and higher saturation pressure. Moreover, the clusters with nanosize gas inclusions are often observed in the areas of higher saturation pressure. The initial period of formation of the embryos' centers for the new phase and further growth of the nanodimensional embryonic particles are characterized by induction periods, which are associated with overcoming certain energies of formation and activation. In accordance with modeling presented in references (Frenkel 1975; Frolov 1982; Sattarov 1999), intensity of formation of the embryos centers for the new phase, J_{n}, (nanodimensional gas inclusions), which is proportional to creation probability and preservation of gas emission centers, has been determined in the following way

$$J_n = A_0 \exp\left(-\frac{\Delta G_n + E_a}{k_B T}\right), \tag{2}$$

Growth intensity of the embryos of a new phase (cluster formation of nanodimensional gas inclusions) is defined as

$$J_g = A_c \exp\left(-\frac{\Delta G_g + E_a}{k_B T}\right), \tag{3}$$

If the embryo of the new phase (gas inclusion) is a spherical form of radius r, a total Gibbs energy of creation and preservation of the gas emission centers ΔG^0 can be written in the following way

$$\Delta G^o = \Delta G_g + E_a = \frac{4}{3}\pi r^3 \frac{U_f - U_g}{V_g} + 4\pi r^2 \sigma. \tag{4}$$

The critical radius, r_c, of the centers of the embryos of the new phase is found by making derivative of ΔG^0 with respect to radius, r, equal to zero. Hence,

$$r_c = \frac{2\sigma V_g}{U_g - U_f}. \tag{5}$$

Based on phase transition kinetics (Frenkel 1975; Frolov 1982; Sattarov 1999), molar volume of the centers of the embryos of the new phase (gas inclusions) can be expressed as

$$V_g = \frac{k_B T}{P_s} \tag{6}$$

Also, difference in chemical potentials of the centers for the embryos of the new phase and of the carrier fluid phase is defined as

$$U_g - U_f = k_B T \ln \frac{P_c}{P_s}. \tag{7}$$

Hence, Equation (5) can be rewritten (assuming negligible difference between critical and saturation densities) as

$$r_c = \frac{2\sigma \frac{k_B T}{P_s}}{k_B T \ln \frac{P_c}{P_s}} = \frac{2\sigma}{P_s \ln \frac{P_c}{P_s}} = \frac{\sigma}{P_s \ln \frac{C_c}{C_s}}. \tag{8}$$

For example, for gas–liquid systems having parameters $\sigma = 1.2 \cdot \times 10^{-3}\, Nm^{-1}$ and $P_s = 3.2\ MP$, it is possible to estimate critical radii of the centers of a new phase of the gas inclusions corresponding to critical pressure $P_c = 6.4\ MPa$ as

$$r_c = \frac{2 \times 1.2 \times 10^{-3}\frac{N}{m}}{6.4 \times 10^{6}\frac{N}{m^2}\ln\frac{6.4MPa}{3.2MPa}} = 0.54 \cdot 10^{-9} m. \tag{9}$$

Thus, under certain conditions, critical hydrodynamic diameters of the centers of embryos for the new phase gas inclusions are nanodimensional, which can then be controlled by changing thermodynamic parameters such as temperature, pressure, and surface tension.

With increase in pressure above the critical value, the gas phase is in the dissolved condition at the molecular level, sizes of which are partially nanodimensional. In an interval of change of pressure between critical and saturation pressures, $P_c > P > P_s$, thermodynamic conditions are created at which there is an intensive growth of embryos of a new phase and cluster formation of nanodimensional gas inclusions occurs. With further decrease of pressure below saturation pressure, the gas phase passes in a free condition. In compliance with the results of experimental research (Sattarov and Farzane 1987; Sattarov 1999), decrease in viscosity to its minimum value occurs in the foregoing area of pressure from critical to saturation pressure $P_c > P > P_s$. So, as far as gas nanoinclusions influence on viscosity characteristics of gas–liquid mixtures, the coefficient of viscosity of a mixture μ_c can be written similarly to Equation (1) as

$$\mu_c = \mu_0(1 + \gamma C), \tag{10}$$

Under isothermal conditions, in the vicinity and above saturation pressure, processes of evolution of gas have nonequilibrium character, and influence of concentration of gas nanoinclusions, C, on the level of pressure, P, can be modeled as (Sattarov and Farzane 1987; Sattarov 1999)

$$\theta\frac{dC}{dt} + C = \beta(P - P_s), \tag{11}$$

On the basis of Equations (10) and (11), it is possible to derive a rheological equation for flow of viscous fluid in a pipe, in the presence of gas nanoinclusions, with the nonlinear parameters depending on level of pressure (Sattarov and Farzane 1987; Sattarov 1999)

$$\theta\frac{d\tau}{dt} + \tau = \beta_* W + \lambda_*\frac{dW}{dt}, \tag{12}$$

where

$$\beta_* = -\frac{4\mu_0}{R_p\gamma}\left[1 + \gamma^2\beta(P - P_s)\right],\ \lambda_* = \theta\frac{\tau}{W}. \tag{13}$$

Similarly, the filtration equation of gas–liquid mixtures with nonlinear parameters, in the vicinity and above saturation pressure, in the presence of gas nanoinclusions, can be modeled (Sattarov et al. 2008) as

$$\vartheta^*\frac{dV}{dt} + V = -\frac{k}{\mu_{0c}}\left(\frac{\partial P}{\partial x} + \theta\frac{d}{dt}\frac{\partial P}{\partial x}\right), \tag{14}$$

where

$$\vartheta^* = \theta\frac{\mu_c}{\mu_{0c}} = -\theta\frac{k}{\mu_{0c}}\frac{\frac{\partial P}{\partial x}}{V},\ \mu_{0c} = \mu_0[1 + \gamma\beta(P - P_s)]. \tag{15}$$

These equations for the flow of viscous fluids in pipes and porous media, in the presence of gas nanoinclusions, can be used in applications to specific engineering problems of regulation of nanodimensions of the gas phase with the objective of increasing efficiency of flow–field systems.

3. Experimental evaluation of gas–liquid mixtures in phase transition regions

The majority of published experimental and theoretical research dedicated to the gas–liquid mixture flows in pipes (Silash 1980; Nigmatulin 1987; Elaouda and Hadj-Taïeb 2013) involves mainly processes at pressures below the saturation pressure. Gas–liquid mixture flows subjected to pressures above or close to the saturation pressure have been, as a rule, researched as homogeneous systems. The basic supposition there has been that the transfer from one state into another happens instantly as in equilibrium thermodynamic theory of phase transformations.

However, as shown above, the state of the gas–liquid mixtures subject to a normal and higher saturation pressure should be analyzed as a situation where gas emission from the liquid and gas dissolution in the liquid occur in a form of embryos (microscopically small gas bubbles), around which continues further growth of a new phase that results in a small growth of pressure (Frenkel 1975).

Our experimental research confirms that the level of the pressure and the rate of its change influence the nano- and microembryos formation in the concentrated volume. Researches of features of these processes have been executed on laboratory installation, consisting of a hermetic cylindrical container with a prepared gas–liquid mixture, a measuring press, a standard pressure gauge, a pressure sensor, an amplifier, a recording instrument, and a thermostat. As a result, experiments have been performed to elucidate the moment of appearance of the nano- and microembryos of the gas phase. Specifically, the gas–liquid mixture consisting of the transformer oil and carbonic acid under the saturation pressure, which is 0.04 MPa, was prepared in a rigid container, joined with a press. Then, the pressure created by the press systematically rose to the point of 0.25 MPa that is significantly above the saturation pressure. After that, the pressure was reduced in a series of steps made at different levels that are above the saturation pressure (Figure 1). These experimental data demonstrate that, beginning with approximately $P = 0.17$ MPa, after each sudden drop of the pressure applied by the press, the pressure of the liquid–gas mixture initially increases. As the level of the press-applied pressure approaches the saturation pressure, the fluid pressure recovery, which is, probably, the result of the formation of the nano- and microembryos of the gas phase, is higher (see Figure 1).

Availability of the nano and microembryos in the fluid system brings forward the issue of dependency of the fluid density on its pressure and the rate of its change and also,

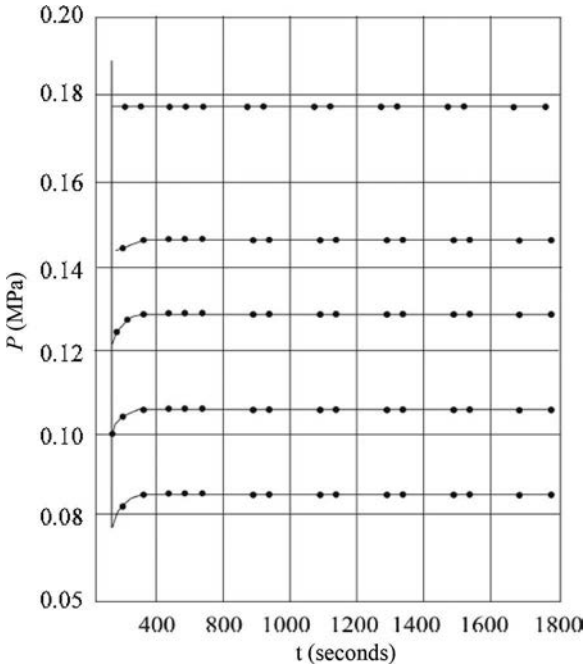

Figure 1. Experimentally obtained time variation of pressure at different levels above the saturation pressure.

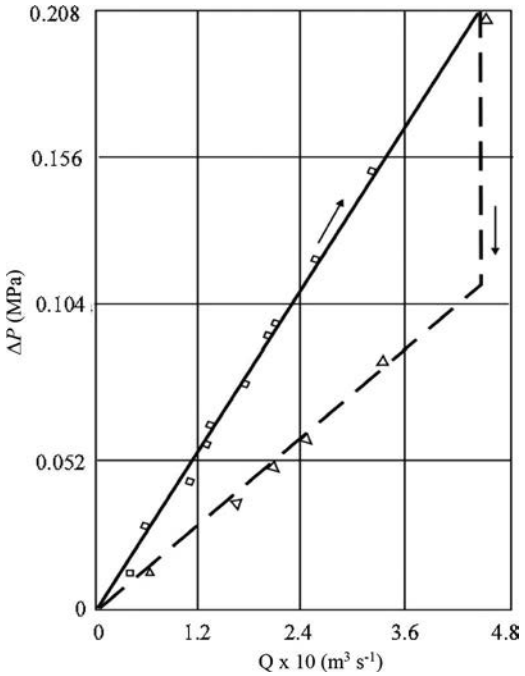

Figure 2. Experimentally obtained relation between pressure drop ΔP of the gas-liquid mixture and its volumetric flow rate Q in a straight circular cross-section pipe (the direction of change of pressure drop is represented by the arrow). □ – measurement of the volumetric flow rate of liquid during the increase of pressure drop; Δ – measurement of the volumetric flow rate of liquid during the decrease of pressure drop.

probably, can explain decrease rheological parameters. For this purpose, an experiment was conducted on an installation consisting of a blender, high-pressure cylinder, pressure sensors, and a pipe 1.3 m long.

Gas–liquid mixture, consisting of transformer oil and carbonic acid, was prepared in the blender. Volume of the liquid phase was $V_l = 0.025 \cdot m^3$, and volume of the gas under the normal conditions was $V_g = 0.0075\ m^3$. Saturation pressure was $P_s = 0.03\ MPa$, and fluid mixture temperature was 293 K. After reaching the saturation pressure, this fluid mixture was kept at that pressure for 60 min.

Then, while keeping the pressure in the blender constant, the pressure difference between this pressure and the pipe exit pressure was continuously increased to $P = 0.15\ MPa$ (without mixing). The volumetric flow rate Q of the effluent mixture was measured during this pressure drop ΔP increase, which was adjusted by the degree of opening of valve (cut-plate) at the pipe exit.

At first, the volumetric flow rate of liquid was measured during the increase of pressure drop. The dependency $Q(\Delta P)$ is depicted as square symbols representing a clearly linear relationship as in the standard case of steady laminar flow of viscous incompressible fluid. Upon reaching the maximum pressure drop (on condition that the pressure at the pipe exit is higher than the saturation pressure), the dependency of $Q(\Delta P)$ was measured during the pressure drop decrease down to almost zero value (Figure 2). In this case, the dependency $Q(\Delta P)$, depicted as triangular symbols in the range of pressure drop between 0.92 and 10.5×10^{-3} MPa, represents another linear relation thus clearly demonstrating a hysteresis anomaly (Figure 2). This phenomenon can be explained by stating that in phase transition regions of liquid–gas mixtures, processes of liberation and dissolution of gas inclusions on nano or micro levels have non-equilibrium character.

4. Modeling of gas–liquid mixtures in phase transition regions

For modeling above mentioned experiments, let us make use of the system of the differential equations for the description of the gas–liquid medium motion in pipes, which generically can be written as (Sattarov 1999)

$$\left.\begin{aligned} \frac{\partial W}{\partial t} + \frac{1}{2}\frac{\partial W^2}{\partial x} &= -\frac{1}{\rho_0}\frac{\partial P}{\partial x} + \frac{\chi}{\rho_0 f_0}\tau(W), \\ \frac{\partial (f\rho)}{\partial t} &= -\frac{\partial (\rho f W)}{\partial x}, \end{aligned}\right\} \tag{16}$$

The system of Equation (16) describes one-dimensional real fluid motion in pipes. First of these equations is actually equation of motion, and the second is continuity equation. For closure system of equations, it is necessary to use a rheological equation and thermodynamic equations of state that are shown below.

The effective cross-section area of the pipe due to pressure and elasticity of pipe is accepted as

$$f = f_0\left(1 + e\frac{P - P_0}{E}\right), \tag{17}$$

where $e = \frac{2R}{\delta_0}$.

In compliance with above-mentioned experiments where it was shown that the new phase formation has noninstant (nonequilibrium) character, relationship between the density and the pressure can be modeled as

$$\frac{\rho_0}{K_c^0}\left(P - P_0 + \theta\frac{\partial P}{\partial t}\right) = \rho - \rho_0 + \frac{K_c^\infty}{K_c^o}\theta\frac{\partial \rho}{\partial t}, \tag{18}$$

Dependency of the shear stress on the averaged velocity for gas–liquid medium can be defined as in the case of laminar steady flow of incompressible viscous fluid in a straight pipe

$$\tau = -\frac{4\mu}{R}W. \tag{19}$$

Viscosity coefficient of the gas–liquid mixture with volumetric concentration, C, of nano- and microdimensional gas inclusions can be modeled in a fashion analog to dependence Equation (10)

$$\mu = \mu_0(1+\gamma_0 C), \tag{20}$$

Here, the value γ_0 can be both positive (for the spherically shaped solid particles, it is accepted as 2.5) and negative (for occluded gas particles). Probably, proportion Equation (20) can be used for the gas–liquid mixture motion, and for pressures below the saturation pressure for the description of bubble conditions.

It can be assumed that the concentration, C, depends on the level of pressure, P, and rate of its change, and also on the nonequilibrium of gas phase formation and dissolution. This allows writing the following phenomenological correlation

$$\theta_c\frac{dC}{dt} + C = \beta_0\left[(P-P_B) + \lambda_p\frac{dP}{dt}\right], \tag{21}$$

which, after integration, yields

$$\begin{aligned} C = {} & \beta_0(P-P_B) - \frac{\beta_0(\theta_c-\lambda_p)}{\theta_c}[P(0)-P_B]e^{-\frac{t}{\theta_c}} \\ & - \frac{\beta_0(\theta_c-\lambda_p)}{\theta_c}\int_0^t e^{-\frac{t-t_1}{\theta_c}}\frac{dP}{dt_1}dt_1. \end{aligned} \tag{22}$$

Equation (16), together with dependencies Equations (17)–(22), forms the full system of the equations of the isothermal motion of the gas–liquid mixture in straight pipes subjected to pressures above and close to the saturation pressure.

If we substitute Equations (17)–(22) into the system of Equation (16), after some transformations (neglecting the nonlinear terms in the equation of continuity), the result will be

$$\left.\begin{aligned} & -\tfrac{1}{\rho_0}\tfrac{\partial P}{\partial x} - \tfrac{1}{2}\tfrac{\partial W^2}{\partial x} = \tfrac{\partial W}{\partial t} + \\ & \quad 2a\Big[1+\beta_0\gamma_0(P-P_B) + \tfrac{\beta_0\gamma_0(\theta_c-\lambda_p)}{\theta_c}[P(0)-P_B]e^{-\frac{t}{\theta_c}} - \\ & \quad - \tfrac{\beta_0\gamma_0(\theta_c-\lambda_p)}{\theta_c}\int_0^t e^{-\frac{t-t_1}{\theta_c}}\tfrac{dP}{dt_1}dt_1\Big]W, \\ & \tfrac{c_\infty^2}{c_0^2}\theta\Big[\tfrac{c^2}{c_\infty^2}\Big(1-\tfrac{c_\infty^2}{c_0^2}\Big)+1\Big]\tfrac{\partial^2 P}{\partial t^2} \\ & \quad + \tfrac{\partial P}{\partial t} = -\rho_0 c^2\Big(\tfrac{\partial W}{\partial x} + \tfrac{c_\infty^2}{c_0^2}\theta\tfrac{\partial^2 W}{\partial t\partial x}\Big), \end{aligned}\right\} \tag{23}$$

where

$$\begin{aligned} 2a = {} & \frac{4\mu_0\chi}{R\rho_0 f_0} = \frac{8\mu_0}{\rho_0 R^2} \\ & \times\left(\frac{f_0}{\chi} = \frac{R}{2}\text{for circular cross section straight pipe}\right); \end{aligned} \tag{24}$$

Here, local speed of sound, c, is defined as

$$c^2 = \frac{K_c^0}{\rho_0\left(1+e\frac{K_c^0}{E}\right)};\ c_\infty^2 = \frac{K_c^\infty}{\rho_0};\ c_0^2 = \frac{K_c^0}{\rho_0}. \tag{25}$$

Estimation of the derivative $\frac{\partial(\rho W f)}{\partial x} = \rho\frac{\partial W f}{\partial x} + W f\frac{\partial \rho}{\partial x} = \rho\frac{\partial W f}{\partial x} + \frac{W f}{c^2}\frac{\partial P}{\partial x}$ in the equation of continuity of system Equation (16) is made as follows. The term $\rho\frac{\partial W f}{\partial x}$ is of the order $\frac{\rho_0 f_0 W}{L}$, and the term $\frac{fW}{c^2}\frac{\partial P}{\partial x}$ is of the order $\frac{f_0 W P}{c^2 L}$. Then, when the first term is much larger than the second term ($\frac{f_0\rho_0 W}{L} >> \frac{f_0 W P}{c^2 L}$, that is, when $\frac{P}{c^2\rho_0} << 1$), the derivative $\frac{\partial(\rho W f)}{\partial x}$ can written as $\frac{fW}{c^2}\frac{\partial P}{\partial x}$.

The last condition is satisfied with the adequate accuracy ($10^{-3} << 1$) for fluids with density $\rho_0 \sim 10^3$ kg m^{-3} under pressure of an order $P \sim 1.0$ MPa and the speed of sound $c \sim 10^3$ m s^{-1}.

Let us now consider steady motion of the gas–liquid mixture under the pressures not below the saturation pressure. In this case,

$$\frac{\partial W}{\partial t} = 0,\ \frac{\partial P}{\partial t} = 0,\ \frac{\partial^2 P}{\partial t^2} = 0,\ \frac{\partial^2 W}{\partial t\partial x} = 0,\ \frac{\partial W^2}{\partial x} = 0. \tag{26}$$

Then, from the second equation of the system Equation (23), it follows that $W =$ constant, while the first equation of this system becomes

$$-\frac{1}{\rho_0}\frac{\partial P}{\partial x} = 2a\left[\begin{aligned} & 1+\beta_0\gamma_0(P-P_B) \\ & \quad - \frac{\beta_0\gamma_0(\theta_c-\lambda_p)}{\theta_c}\int_0^t e^{-\frac{t-t'}{\theta}}\frac{dP}{dt'}dt' \end{aligned}\right]W. \tag{27}$$

Taking into account the chain-rule expression for the total derivative

$$\frac{dP}{dt'} = \frac{\partial P}{\partial t'} + \frac{dx}{dt'}\frac{\partial P}{\partial x} = \frac{\partial P}{\partial t'} + W\frac{\partial P}{\partial x} \tag{28}$$

and taking into consideration the stationary condition, $\frac{\partial P}{\partial t'} = 0$, the Equation (27) becomes

$$-\frac{1}{\rho_0}\frac{\partial P}{\partial x} = 2a\left[\begin{aligned} & 1+\beta_0\gamma_0(P-P_H) \\ & \quad - \frac{\beta_0\gamma_0(\theta_c-\lambda_p)}{\theta_c}W\int_0^t e^{-\frac{t-t'}{\theta_c}}\frac{dP}{dx}dt' \end{aligned}\right]W. \tag{29}$$

Differentiation of the Equation (29), taking into account that $\frac{d}{dt} = W\frac{d}{dx}$, results in

$$\begin{aligned} -\frac{1}{\rho_0}W\frac{d^2P}{dx^2} = {} & 2a\beta_0\gamma_0 \\ & \times\left(W\frac{dP}{dx} + \frac{\theta_c-\lambda_p}{\theta_c^2}W\int_0^t e^{-\frac{t-t'}{\theta_c}}\frac{dP}{dx}dt' - \frac{\theta_c-\lambda_p}{\theta_c}W\frac{dP}{dx}\right)W. \end{aligned} \tag{30}$$

After some transformations, using Equation (29), the Equation (30) can be written as a second-order ordinary differential equation

$$\theta_c \frac{d^2P}{dx^2} + \left(2a\beta_0\gamma_0\lambda_p\rho_0 W + \frac{1}{W}\right)\frac{dP}{dx} + 2a\beta_0\gamma_0\rho_0 P = 2a\gamma_0\beta_0\rho_0 P_H - 2a\rho_0. \quad (31)$$

with initial conditions

$$P(0) = P^{\circ},\ \frac{dP(0)}{dx} = 2a\rho_0 W. \quad (32)$$

Analytic solution of differential Equation (31) subject to initial conditions Equation (32) is

$$P = P_B - \frac{1}{\gamma_0\beta_0} - \frac{1}{K_1 - K_2} \times \left[\left(P^0 - P_B + \frac{1}{\gamma_0\beta_0}\right) \times \left(K_2 e^{K_1 x} - K_1 e^{K_2 x}\right) + 2a\rho_0 W\left(e^{K_1 x} - e^{K_2 x}\right)\right], \quad (33)$$

$$K_{1,2} = \frac{-\left(2a\gamma_0\beta_0\lambda_p\rho_0 W + \frac{1}{W}\right) \pm \sqrt{\left(2a\gamma_0\beta_0\lambda_p\rho_0 W + \frac{1}{W}\right)^2 - 4\cdot 2a\gamma_0\beta_0\rho_0\theta_c}}{2\theta_c}. \quad (34)$$

In the case when $x = L$, $P(L) = P_L$ and $K_i\ L << 1$, typical for the short pipelines and large times of nonequilibrium, relation Equation (33) after some transformations gives pressure drop as

$$\Delta P = P^o - P_L = 2a\rho_0 WL\left(1 - 2a\gamma_0\beta_0\rho_0 WL\frac{\lambda_p}{2\theta_c}\right) + (P^0 - P_B)\frac{2a\gamma_0\beta_0\rho_0 L^2}{2\theta_c}. \quad (35)$$

This equation demonstrates that availability of nano- and microembryos of the new gas phase in the gas–liquid mixture results in lowering of the pressure drop, and, if the value of times of nonequilibrium θ_c grows, this effect decreases.

In the case when $x = L$, $P(L) = P_L$ and $K_i\ L >> 1$, typical for the long pipelines and sufficiently small times of nonequilibrium, Equation (33) after some transformations gives pressure drop as

$$\Delta P = 2a\rho_0 WL - \frac{1}{\gamma_0\beta_0} + P_B - P_L. \quad (36)$$

So, the pressure loss in gas–liquid systems in long straight pipes depends on the values of pressures P_B, P_L and coefficients γ_o, β_o, characterizing availability of occluded gas bubbles in the system. If $\frac{1}{\gamma_0\beta_0} + P_L > P_B$, pressure loss in such a gas–liquid system is less in comparison with pressure loss in a homogeneous medium. In case of $\frac{1}{\gamma_0\beta_0} + P_L < P_B$, pressure drop in such a gas–liquid system exceeds pressure loss in a homogeneous medium.

These conclusions confirm the corresponding experiments for similar conditions shown in (Bolotov et al. 1988; Sattarov 1999, 2012; Mirzadzhanzade et al. 1999, 2003), where it was established that when pressure considerably exceeds the saturation pressure, the increase of specific rate of solution is observed, proceeding with pressure decrease before achieving the saturation pressure.

Equation (27) is used for the description of experimental data in Figure 2. Let us assume that the rate of change of pressure stayed constant, that is, $\frac{dP}{dt} = A = const$ during the experiments. Then, taking into consideration the stationary conditions of making the experiments, Equation (27), after some transformations, results in

$$-\frac{1}{\rho_0}\frac{dP}{dx} = 2a\left[1 + \beta_0\gamma_0(P - P_H) - A\beta_0\gamma_0(\theta_c - \lambda_p)\right]W \quad (37)$$

or

$$\frac{dP}{dx} + 2a\rho_0\beta_0\gamma_0 WP = 2a\rho_0 W\left[1 - \beta_0\gamma_0 P_H - A\beta_0\gamma_0(\theta_c - \lambda_p)\right]. \quad (38)$$

Analytic solution of the Equation (38) under condition $P(0) = P^o$ is

$$P = \left\{P^0 + \frac{1}{\beta_0\gamma_0}\left[1 - \beta_0\gamma_0 P_H - A\beta_0\gamma_0(\theta_c - \lambda_p)\right]\right\} \times e^{-2a\rho_0\beta_0\gamma_0 Wx} - \frac{1}{\beta_0\gamma_0}\left[1 - \beta_0\gamma_0 P_H - A\beta_0\gamma_0(\theta_c - \lambda_p)\right]. \quad (39)$$

As $x = L$, $P(L) = P_L$ and taking into account that $2\alpha\rho_o\beta_o\gamma_o WL << 1$ is carried out in laboratory conditions, Equation (39) gives the following expression for the pressure drop

$$\Delta P = P^0 - P_L = 2a\rho_0 WL\left[1 + \beta_0\gamma_0(P^0 - P_B) - A\gamma_0\beta_0(\theta_c - \lambda_p)\right]. \quad (40)$$

Analysis of relationship Equation (40) shows that the pressure drop depends not only on gas content but also the rate of pressure change in the fluid mixture system. So, as the pressure decreases with time ($A < 0$), the pressure drop will be somewhat higher than the pressure drop in the case when pressure increases with time ($A > 0$).

Experimental data given in Figure 2 were fitted with Equation (40) resulting in the following values of parameters:

$$\mu_0 = 16.9Pa\cdot s,\ \rho = 880\frac{kg}{m^3},$$
$$L = 1.3m,\ P^0 = 0.15MPa,\ P_B = 0.16MPa,$$

$$\left|\frac{dP}{dt_1}\right| = |A| = 2.85\cdot 10^{-2} MPa/s.$$

As a result, it is possible to calculate the group of terms $2\alpha\rho_0 W = 5.51\cdot 10^{-2}$ MPa/m.

Using this calculated value for $2\alpha\rho_0 W$, two values of $\frac{\Delta P}{W}$ can be calculated for different sign of rate of pressure change as

$$A < 0,\ \frac{\Delta P}{W} = 5.5\cdot 10^{-2}(MPa/m)s$$
$$A > 0,\ \frac{\Delta P}{W} = 3.25\cdot 10^{-2}(MPa/m)s.$$

These values can then be used to evaluate parameters from Equation (40)

$$\beta_0\gamma_o = 2 \cdot 10^{-1} 1/MPa\ \theta_c - \lambda_P = 72\ s.$$

These results of these calculations on the basis of relationship Equation (40) are depicted in Figure 2 as dashed straight lines, which correlate well with experimental data. Furthermore, comparing the experimental results with the analytical research shows that indeed, under certain conditions above the separation pressure levels, dynamically stable embryos of a new phase are formed on nano level or micro level (Bolotov et al. 1988; Mirzadzhanzade et al. 1999; Sattarov 1999, 2012; Houshmand et al. 2014). This demonstrates that the proposed nanomodels of flow and filtration presented in this paper reliably describe the phenomenon of reduction of the effective viscosity of gas–liquid systems in the transition areas above the saturation pressure (Sattarov and Farzane 1987; Bolotov et al. 1988; Mirzadzhanzade et al. 1999; Sattarov 1999). This proves that Einstein's model for effective viscosity of mixtures (Eq. 1) should be generalized for use in gas–liquid mixtures.

5. Conclusions

Some features of a gas–liquid mixture in areas of transition of a phase are studied. It has been thermodynamically proven and established that the gas–liquid systems undergoing phase transformation in the initial stage consist of nanoparticles or clusters of nanoparticles that differ from the usual small size of microscopic inclusions in the aggregation state of the corresponding phase. On the basis of the thermo-hydrodynamic analysis of gas–liquid systems undergoing phase transition, useful equations have been derived applicable to filtration in the porous media and flows in straight pipes. The experimental research on gas–liquid systems in the concentrated volume has shown that the level of pressure and the time-rate of its change influence the nano- and microembryos formation in areas of phase transition. Experiments have also been performed to define the moment of nucleation inception of the nano- and microembryos of the gas phase and to determine their growth during time. The experimental research on motion of a gas–liquid system in straight pipes has established that dependency of volumetric flow rate of mixture on the pressure drop in a pipe has a nonequilibrium character with apparent strong hysteresis. Theoretical calculations of motion of gas–liquid mixtures in straight pipes involving phase transition regions were carried out. The results of theoretical calculations on the basis of the suggested mathematical model have demonstrated excellent agreement with experimental data. This analytical and experimental research has shown that nonequilibrium thermo-hydrodynamic models are capable of describing processes in phase transition regions that exist in moving gas–liquid systems in the porous medium and straight pipe flows. In application extension, the results obtained and the proposed nanomodels for flow and filtration of gas–liquid systems in pretransition and transition saturation fields can be used to solve specific engineering problems to improve the efficiency of different technological processes in chemical and gas- and oil-producing industries. Additional practical application of this theory would be its extension to the elucidation of well-known drag force reduction effect on objects in liquid flows when injecting microbubbles through the surface of the object.

Nomenclature

A_0, A_c	coefficients of proportionality (s^{-1})
c	speed of sound (ms^{-1})
C	concentration parameter of dispersed phase; concentration of gas nanoinclusions (total volume of nanoinclusions per total volume of the mixture)
C_c	concentration of the centers of the embryos of new phase with critical radiuses r_c
C_s	concentration of gas inclusions under saturation pressure (concentration of the liquid inclusions at the condensation pressure in condensation process)
E_a	activation energy of viscous flow (Nm)
E	modulus of elasticity of the pipe material (Nm^{-2})
f	cross-section area (m^2)
f_0	cross-section area under the pressure P_0 (m^2)
ΔG_g	Gibbs free energy of formation of the clusters for the new phase embryos (Nm)
ΔG_n	Gibbs free energy of formation of the embryos centers for the new phase (Nm)
J_n	intensity of formation of the embryo centers for the new phase (s^{-1})
J_g	growth intensity of the embryos of a new phase (cluster formation of gas inclusions) (s^{-1})
K_c^0	modulus of volume pressing of the systems during very slow processes (Nm^{-2})
K_c^∞	modulus of volume pressing of the systems during quick-passing processes (Nm^{-2})
k	permeability of porous medium (m^2)
k_B	Boltzmann constant ($Nm\ K^{-1}$)
L	length of a pipeline section (m)
P	pressure (Nm^{-2})
P_c	critical pressure, under which the centers of the embryos of new phase with critical radii, r_c, are formed (Nm^{-2})
P_s	saturation pressure (in processes of condensation, it is called condensation pressure) (Nm^{-2})
P_B	pressure of the formation of gas nano- and microembryos in liquid (Nm^{-2})
$\frac{\partial P}{\partial x}$	pressure gradient for filtration of gas–liquid mixture in the presence of gas nanoinclusions (Nm^{-3})
Q	volumetric flow rate of gas–liquid mixture ($m^3\ s^{-1}$)
R	pipe radius (m)
r	radius of the centers for the embryos of new phase (gas inclusions) (m)
r_c	critical radius of the centers for the embryos of new phase (gas inclusions) (m)
T	absolute temperature (K)
t	time (s)
U_f	chemical potential of the carrier fluid phase (Nm)
U_g	chemical potential of the centers for the embryos of new phase (Nm)
V_g	molar volume of the centers for the embryos of new phase (gas inclusions) (m^3)

W averaged velocity for flow of viscous fluid in a pipe, in the presence of gas nanoinclusions (ms^{-1})
x flow direction (m)

Greek Symbols

β coefficient of solubility of gases in fluid ($N^{-1}\,m^2$)
β_0 constant (as far as the processes are considered under the pressures $P \le P_B$, then $\beta_0 < 0$) ($N^{-1}m^2$)
γ, γ_0 constant coefficient
δ_0 walls thickness (m)
θ, θ_c,λ_p characteristic times for formation of gas inclusions in gas–liquid mixture (s)
ρ density of the medium ($kg\,m^{-3}$)
ρ_0 density under the pressure P_0 ($kg\,m^{-3}$)
μ, μ_c viscosity of the dispersed systems; viscosity of the heterogeneous system ($N\,s\,m^{-2}$)
μ_0 viscosity of the continuum; viscosity of a fluid ($Ns\,m^{-2}$)
σ surface tension of the centers for the embryos of new phase (gas inclusions) (Nm^{-1})
τ viscous deviator part of the stress tenor (Nm^{-2})
χ wetted perimeter (m)

Subscripts

n new
a activation
g gas
c critical
s saturation

Acknowledgments

The views and conclusions contained herein are those of the authors and should not be interpreted as necessarily representing the official policies or endorsements, either expressed or implied, of the Naval Surface Warfare Center, US Department of Energy/NETL or the U.S. Government. The U.S. Government is authorized to reproduce and distribute reprints for government purposes notwithstanding any copyright notation thereon.

Funding

This research was partially supported by the Naval Surface Warfare Center, Panama City Division, Florida under the supervision of Dr. Frank J. Crosby and facilitated by Dr. Quyen Huynh via TriCircle Company. It was also partially supported by the Department of Energy's National Energy Technology Laboratory under grant number DE-FE0023114 to FIU/ARC.

References

Bolotov, A. A., A. K. Mirzadzhanzade, and I. I. Nesterov. 1988. Rheological properties of solutions of gases and a liquid in saturation pressure regions. *Proceedings of Academy of Sciences of the USSR, FGM*, N 1, 143–46.

Clasen, C., and G. H. McKinley. 2004. Gap-dependent microrheometry of complex liquids. *Journal of Non-Newtonian Fluid Mechanics* 124:1–10. doi:10.1016/j.jnnfm.2004.07.015.

Einstein, A. 1966. *Collection of scientific works*. Moscow: Nauka, tom. 3, 632.

Elaoud, S., and E. Hadj-Taïeb. 2013. Gas-liquid transient flow analysis in deformable pipes. *International Journal of Current Engineering and Technology* 3 (4):1367–74.

Frenkel, J. I. 1975. *Kinetic theory of liquids*. Moscow: Nauka, 592.

Frolov, Y. 1982. *Course of colloidal chemistry*. Moscow: Chemistry, 400.

Havkin, A. J. 2007. Nanotechnology in an oil production. *Oil Industry* 6:58–60.

Houshmand, F., D. Elcock, M. Amitay, and Y. Peles. 2014. Bubble formation from a micro-pillar in a microchannel. *International Journal of Multiphase Flow* 59:44–53. doi:10.1016/j.ijmultiphaseflow.2013.10.011.

Mirzadzhanzade, A. H., M. M. Hasanov, and R. N. Bahtizin. 1999. *Studies about modelling of complicated systems for oil production*. Ufa, Russia: Gliem, 464.

Mirzadzhanzade, A. K., O. L. Kuznetsov, K. S. Basniev, and Z. S. Aliev. 2003. *Foundation of gas recovery technology*. Moscow: Nedra, 880.

Mirzadzhanzade, A. H., F. G. Maksudov, R. I. Nigmatulin, and R. M. Sattarov. 1985. *Theory and practice of application of nonequilibrium systems in oil production*. Baku, Azerbaijan: Elm, 220.

Nigmatulin, R. I. 1987. *Dynamics of multiphase medium*. Moscow: Nauka, (I, II), 464, 360.

Sattarov, R. M. 1999. *Nonsteady movement of rheologically complicated liquids in pipes*. Baku, Azerbaijan: Elm, 412.

Sattarov, R. M., G. S. Dulikravich, M. I. Kurbanbaev, I. R. Sattarzada, A. Z. Abitova, M. A. Nugiev, and B. T. Muhambetov. 2012. Certain specifics of nanomodelling of rheologically complex fluid mixtures. *Proceedings of Khazarneftgazyatag–2012* Scientific-Practical Conference, Baku, Azerbaijan, December 4–5.

Sattarov, R. M., M. M. Ermekov, V. N. Babashev, and M. N. Babasheva. 2008. *Towards a substantiation of relaxation filtration models for liquid–gas systems*. Atyrau: Bulletin AIOG, No. 1, 54–57.

Sattarov, R. M., and P. J. Farzane. 1987. Motion of gas-liquid systems, taking account of micronucleus formation. *Journal of Engineering Physics and Thermophysics* 52 (5):555–61. doi:10.1007/bf00873309.

Sattarov, R. M., I. R. Sattarzada, S. I. Bakhtiyarov, and R. N. Ibragimov. 2016. Modeling of complex rheological fluids with fractal structures. *An Interdisciplinary Journal of Discontinuity, Nonlinearity and Complexity* 5 (3):199–207. doi:10.5890/dnc.2016.09.001

Sattarov, R. M., I. R. Sattarzada, and A. G. Gusmanova. 2010. *Nanosimulation of the development and exploitation operating procedures of oil and gas fields*. Vestnik CKR Rosnedra, No. 2, pp. 59–67.

Silash, A. P. 1980. *Extraction and transportation of oil and gas. Part I, II*. Moscow: Nedra, 376, 264.